s,t,u,v intermediate length values used to determine beam area ratios
W_c collector width
W_r reflector width
X_c collector width ratio
α solar altitude angle
α_{EW} solar altitude angle projected in the east-west plane
α_{NS} solar altitude angle projected in the north south plane
β_c collector tilt angle
β_r reflector tilt angle
γ solar azimuth angle
ρ_g ground reflectance
ρ_r reflector reflectance
ϕ latitude
$\bar{\omega}$ hour angle

REFERENCES

Chiam H. F. Planar concentrators for flat plate solar collectors. *Solar Energy* **26**, 503–509 (1981).

Chiam H. F. Stationary reflector-augmented flat-plate collectors. *Solar Energy* **29**, 65–69 (1982).

Collares-Pereira M. and Rabl A. The average distribution of solar radiation-correlation between diffuse and hemispherical and between daily and hourly insolation values. *Solar Energy* **22**, 155–164 (1979).

Duffie J. A. and Beckman W. A. *Solar Engineering of Thermal Processes*, 2nd edn. Wiley–Interscience, New York (1991).

Grassie S. L. and Sheridan N. R. The use of planar reflectors for increasing the energy yield of flat-plate collectors. *Solar Energy* **19**, 663–668 (1977).

Grimmer D. P., Zinn K. G., Herr K. C. and Wood B. E. Augmented solar energy collection using different types of planar reflective surfaces: theoretical calculations and experimental results. *Solar Energy* **21**, 497–501 (1978).

Jones R. E. Radiation on reflector augmented collector rows tilted toward the equator. *Solar Energy* **33**, 527–531 (1984).

Larson D. C. Mirror enclosures for double-exposure solar collectors. *Solar Energy* **23**, 517–524 (1979).

Larson D. C. Concentration ratios for flat-plate solar collectors with adjustable flat mirrors. *J. Energy* **4**, 170–175 (1980a).

Larson D. C. Optimization of flat-plate collector-flat mirror systems. *Solar Energy* **24**, 203–207 (1980b).

Liu B. Y. H. and Jordan R. C. The long-term average performance of flat-plate solar energy collectors. *Solar Energy* **7**, 53–75 (1963).

McDaniels D. K., Lowndes D.H., Mathew H., Reynolds J. and Gray R. Enhanced solar energy collection using reflector-solar thermal collector combinations. *Solar Energy* **17**, 277–283 (1975).

National Renewable Energy Laboratory. National Solar Radiation Database, National Climatic Data Center, Asheville, N.C. (1992).

Perers B. and Karlsson B. External reflectors for large solar collector arrays, simulation model and experimental results. *Solar Energy* **51**, 327–337 (1993).

Perez R., Seals R., Ineichen P., Stewart R. and Menicucci D. A new simplified version of the Perez diffuse irradiance model for tilted surfaces. *Solar Energy* **39**, 221 (1987).

Rao A. V. N., Chalam R. V., Subramanyam S. and Rao T. L. S. Energy contribution by booster mirrors. *Energy Conserv. Mgmt.* **43**, 309–326 (1993).

Reindl D. T., Beckman W. A. and Duffie J. A. Evaluation of hourly tilted surface radiation models. *Solar Energy* **45**, 9–17 (1990).

Rudloff F. A., Swanson S. R. and Boehm R. F. Computer simulation results for planar reflectors and flat plate solar collectors. ASME Paper 79-WA/Sol-37, *ASME Winter Annual Meeting*, New York (1979).

Seitel S. C. Collector performance enhancement with flat reflectors. *Solar Energy* **17**, 291–295 (1975).

Sparrow E. M. and Cess R. D. *Radiation Heat Transfer*. Brooks/Cole, Calif. (1966).

Tabor H. Stationary mirror systems for solar collectors. *Solar Energy* **2**, 27–33 (1958).

Tabor H. Mirror Boosters for solar collectors. *Solar Energy* **10**, 111–118 (1966).

Taha I. S. and Eldighidy S. M. Effect of off-south orientation on optimum conditions for maximum solar energy absorbed by flat plate collector augmented by plane reflector. *Solar Energy* **25**, 373–379 (1980).

Pergamon

0038-092X(95)00060-7

Solar Energy Vol. 55, No. 5, pp. 355–362, 1995

0038-092X/95 $9.50+0.00

ON THE GROUND TEMPERATURE BELOW BUILDINGS

G. MIHALAKAKOU,† M. SANTAMOURIS, D. ASIMAKOPOULOS and A. ARGIRIOU

University of Athens, Department of Applied Physics, Laboratory of Meteorology, 33 Ippokratous str., 106 80 Athens, Greece

(Communicated by J. OWEN LEWIS)

Abstract—A transient, numerical model for the prediction of the ground temperature at various depths below buildings is presented in this paper. The proposed model was developed by calculating the heat flow to the ground from a building, which depends on the complicated three-dimensional thermal process in the ground. The main difficulties in obtaining manageable solutions of the heat flow problem were: The three-dimensionality of the thermal process, the strong temporal variability of the outdoor temperature as well as the large number of parameters involved in describing the building foundation geometry as well as the thermal insulation. The techniques of superposition and numerical analysis were used to cope with these difficulties. The model was validated against experimental data and it was found that it could accurately predict the ground temperature under a building.

1. INTRODUCTION

The demand for more precise methods to calculate heating and cooling load of a building has been increased during the last two decades and has led to many studies of the transient heat flow from a building foundation to the ground.

The use of direct or indirect earth coupling techniques for buildings requires knowledge of the ground temperature profile below the building foundation. The direct earth contact involves partial or total placing of the building envelope in direct contact with the soil while the indirect contact involves the use of an earth-to-air heat exchanger system, (Mihalakakou *et al.*, 1994a; Mihalakakou *et al.*, 1994b; Santamouris *et al.*, 1995), through which air from the building or from the outside is circulated and then is brought into the building.

The different calculation models, which were developed to predict the ground temperature under a building, are based on analytical solutions, on numerical analysis and experimental measurements. An important number of papers deal with a two-dimensional steady state heat flow process (Billington, 1951; Vuorelainen, 1960a,b; Landman and Delsante, 1987. Moreover, an extensive analysis of the heat flow processes in order to obtain sufficiently accurate, analytical and as simple as possible formulae, for the heat flow has been described by Claesson and Eftring (1980), Claesson and Dunand (1983), Hagentoft (1988a), and by Claesson and Hagentoft (1991).

Fourier analysis and transformation were used in Muncey and Spencer (1977) and in Delsante *et al.* (1983) to obtain expressions for the heat from uninsulated slabs. The boundary temperatures varied periodically with time while the temperature change under the walls, at the level of ground, was assumed to be linear.

Delsante (1988) derived an analytical expression for the two-dimensional steady state heat loss from a slab on the ground with the same thermal resistance at the ground surface and the floor. The temperature under the wall at the ground level was assumed to change linearly. A similar technique has been described in Hagentoft (1988b) and in Delsante (1989) while a method for calculating the heat loss of cellars was developed by Kusuda and Bean (1984).

The temperature under a building foundation was numerically calculated for steady state cases by Adamson *et al.* (1973) and Backstrom *et al.* (1985).

Boileau and Latta (1968) developed a simplified method to calculate heat flow for uninsulated cellars. The results of this simplified method were compared with numerical predictions by Shipp and Broderick (1980) and it was found in a very good agreement for uninsulated building foundation.

Mitalas (1982) developed a two-dimensional model for calculating the heat flow process for cellars. He divided the cellar wall and floor in five segments assuming that the outdoor temperature varied periodically.

†To whom all correspondence should be addressed at: Energy Research Group, University College Dublin, Richview Clonskeagh Drive, Dublin 14, Ireland.

Kusuda *et al.* (1983) described a calculation model in which the ground surface was divided in rectangular segments. The segment's temperature varied periodically. The thermal problem was solved integrating the Green's function solution.

However, a large number of these methods are characterised by limited applicability as they do not take into account the three-dimensionality of the heat flow thermal process as well as the strong temporal variation of the outdoor temperature.

The present paper deals with the rather complicated thermal process in the ground under a building and, in particular, with the heat flow through the foundation. The main goal was to obtain an accurate method to calculate the heat flow to the ground and thus the ground temperature below a building foundation at various depths. The present method can be used for a wide range of applications, such as the direct contact buildings as well as the indirect contact technique, and it can be easily used for the accurate prediction of the ground temperature profile when an earth-to-air heat exchangers' system has been buried under a building. In this case, the ground temperature at a certain point in the pipe vicinity should be estimated by the superposition of the ground temperature caused by the heat exchanger presence and of the ground temperature caused by the ground surface boundary conditions.

2. MODELLING OF GROUND TEMPERATURE UNDER A BUILDING

The thermal problem of the heat flow from a building to the ground presents various difficulties caused by the genuinely three-dimensional, time-dependent character of the heat flow process in the ground below and around the building. The ground temperature $T(x,y,z,t)$ can accurately be modelled (Carslaw and Jaeger, 1959) by the following three-dimensional, transient, heat conduction equation:

$$\rho C_p(\partial T/\partial t)=\nabla(K\nabla T) =\partial/\partial x(K\partial T/\partial x)+\partial/\partial y(K\partial T/\partial y) +\partial/\partial z(K\partial T/\partial z) \quad (1)$$

where ∇ indicates the gradient operator.

The heat flux in the ground can be written as follows:

$$-K\nabla T=-K(\partial T/\partial x,\partial T/\partial y,\partial T/\partial z). \quad (2)$$

The total heat flow $Q(t)$ from the building to the ground can be stated as follows:

$$Q(t)=\int\int_{S_i}-K\nabla T n dS. \quad (3)$$

Here n denotes the unit normal to S_i pointing from ground to building.

The initial condition is the following:

$$T(x, y, z, t=0)=T_s(z) \quad (4)$$

where $T_s(z)$ was considered to be the undisturbed ground temperature. In order to solve the differential eqn (1) we assume that at $t=0$ there is not any influence from the building's presence.

The boundary conditions are:

(1) Co-ordinate x

at $x=x_a$:

$$T(x=x_a, y, z, t)=T_u(z) \quad (5)$$

at $x=x_b$:

$$T(x=x_b, y, z, t)=T_u(z) \quad (6)$$

where, x_a and x_b are two large axial distances from the building foundation which were taken equal to 100 m. At those distances (x_a, x_b) the temperature distribution is not influenced by the heat flow caused by the building presence. Thus, the temperature at x_a and x_b is the undisturbed soil temperature. $T_u(z)$ is the undisturbed ground temperature at a certain depth z which does not change with time and is not influenced by the building's presence.

(2) Co-ordinate y

at $y=y_a$:

$$T(x, y=y_a, z, t)=T_u(z) \quad (7)$$

at $y=y_b$:

$$T(x, y=y_b, z, t)=T_u(z). \quad (8)$$

Similarly, y_a and y_b are two large distances in the y-direction where the temperature distribution is not influenced by the building's presence.

(3) Co-ordinate z

at $z=0$ (at the ground surface):

$$T(x, y, z=0, t)=T_{boundary} \quad (9)$$

where, $T_{boundary}$ was equal to the constant indoor surface temperature (T_i) for the case of the foundation interior region while for the case of the ground surface $T_{boundary}$ was equal to the outdoor temperature $(T_{out}(t))$.

at $z=z_c$:

$$T(x, y, z=z_c, t)=T_u(z_c) \quad (10)$$

where, z_c was a large vertical distance in the soil, taken equal to 50 m, where the soil temperature was considered to be the undisturbed soil temperature.

Furthermore, the superposition technique was used to analyse the outdoor temperature variation. Thus, the principle of superposition for this case was illustrated in Fig. 1 and for two superimposed components (1) and (2).

The outdoor temperature at the ground surface can be represented (Carslaw and Jaeger, 1959; Mihalakakou *et al.*, 1992) by a Fourier series:

$$T_{out}(t)=T_0+\sum_{n=1}^{\infty}T_n\sin(2\pi nt/t_p+\lambda_n). \quad (11)$$

The two first harmonics of the eqn (11) have been used in this study in order to calculate the outdoor temperature at the ground surface. The thermal conductivity values used in this study were obtained from Puri (1986) and Gee (1966), while the soil density (ρ) and the soil specific heat capacity (C_p) were taken from Puri (1986). The transient building-ground system described in this paper incorporates four independent (x, y, z, t) and one dependent variables (T). The numerical method of control volume formulation was used to discretize the three-dimensional differential eqn (1). This method (Patankar, 1980), which can be regarded as a special and new version of the method of weighted residuals, looks like the finite-difference method but it employs many ideas that are typical of the finite element methodology.

The first step in the control volume formulation was to divide the calculation domain into a finite number of control volumes. A portion of a two-dimensional grid was shown in Fig. 2. For the grid point P, points E and W were its x-direction neighbours, while N and S are the y-direction neighbours. The control volume around P was shown by dashed lines. Finally, and for the present three-dimensional problem, two more neighbours T and B were added for the z-direction to complete the three-dimensional configuration.

Moreover, it has been considered that the grid points were located at the geometric centre of each control volume. This location was presented in Fig. 3 for a two-dimensional problem. The discretization equation was derived by integrating the differential eqn (1) over each control volume and over the time interval from t to $t+\Delta t$. The order of this integration was chosen according to the nature of the term. For the representation of the terms $\Delta T/\Delta t$ was assumed that the grid point values of T prevail through the control volume. As it regards the terms $\Delta T/\Delta x$, $\Delta T/\Delta y$ and $\Delta T/\Delta z$, it was necessary to make a profile assumption or an interpolation formula. The simplest possibility was to assume that the value of T at a grid point prevails over the control volume surrounding it. For this profile, the slope $\Delta T/\Delta x$ was not defined at the control volume faces. A profile which does not suffer from this difficulty is the piece-wise linear profile. In this study, linear interpolation functions were used between grid points.

The time dependency was best handled

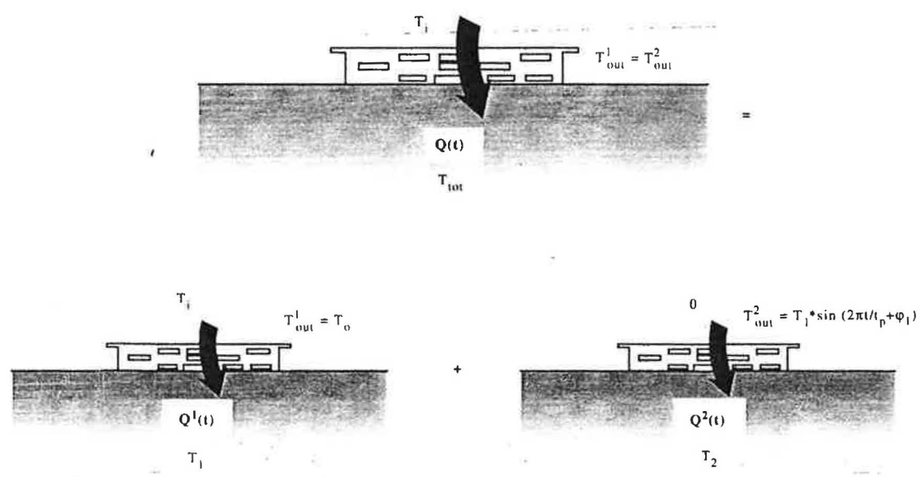

Fig. 1. The technique of superposition where the temperature at the ground surface was divided in two components (1) and (2).

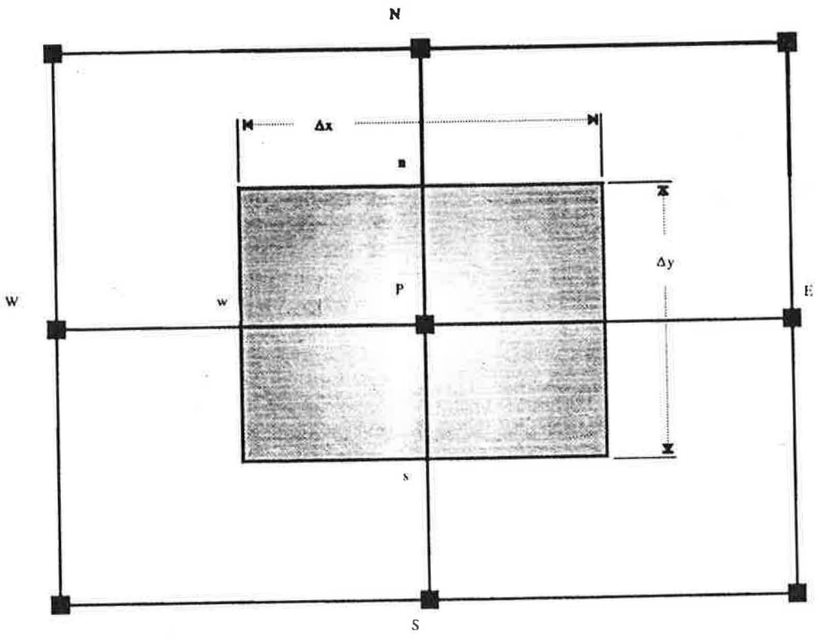

Fig. 2. Control volume for two-dimensional situation.

using implicit integration techniques. The fully implicit scheme satisfies the requirements of simplicity and physically satisfactory behaviour. Therefore, the discretization equation can easily be seen after the integration of the differential eqn (1) as follows:

$$\alpha_P T_p = \alpha_E T_E + \alpha_W T_W + \alpha_N T_N + \alpha_S T_S + \alpha_T T_T + \alpha_B T_B + b \quad (12a)$$

where:

$$\alpha_E = K_e \Delta y \Delta z/(\delta x)_e \quad (12b)$$

$$\alpha_W = K_W \Delta y \Delta z/(\delta x)_w \quad (12c)$$

$$\alpha_N = K_n \Delta z \Delta x/(\delta y)_n \quad (12d)$$

$$\alpha_S = K_S \Delta z \Delta x/(\delta y)_s \quad (12e)$$

$$\alpha_T = K_t \Delta x \Delta y/(\delta z)_t \quad (12f)$$

$$\alpha_B = K_b \Delta x \Delta y/(\delta z)_b \quad (12g)$$

$$\alpha_P^0 = \rho C_p \Delta x \Delta y \Delta z/\Delta t \quad (12h)$$

$$b = \alpha_P^0 T_P^0 \quad (12i)$$

$$\alpha_P = \alpha_E + \alpha_W + \alpha_N + \alpha_S + \alpha_T + \alpha_B + \alpha_P^0. \quad (12j)$$

The neighbours coefficients α_E, α_W, α_N,..., α_B represent the conductance between the point P and the corresponding neighbour while the term $\alpha_P^0 T_P^0$ is the internal energy contained in the control volume at time t.

In this study the whole system of the algebraic equations presented by eqn (12) were solved using the Gauss–Seidel iterative method, according to this method the values of the variables were calculated using each grid point in a certain order.

This numerical method can be regarded as the best way to handle the serious difficulty of the large number of parameters involved in describing the foundation geometry and the thermal insulation. Therefore, considering a big number of control-volumes it was easier to specify the size and the shape of the foundation surface, the thickness of a thermal insulation and its thermal conductivity.

The whole program was developed inside TRNSYS environment. TRNSYS (1990), is a transient system simulation program with a modular structure which facilitates the addition to the program of other mathematical models not included in the standard TRNSYS library. The time step for the TRNSYS simulations was taken equal to 0.1 h.

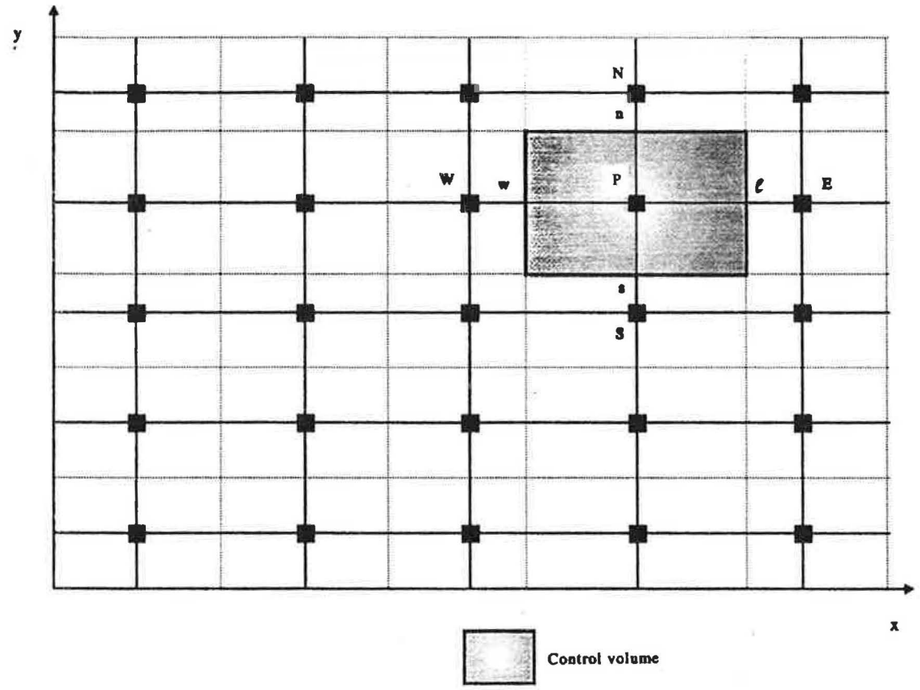

Fig. 3. Location of the control volume faces.

3. MODEL VALIDATION

The collection and analysis of a comprehensive set of experimental data was considered an essential part of this research in order to provide a basis for the verification of the accuracy of the mathematical model.

For this purpose, two experiments were carried out during the summer. Each experiment lasted 20 days, 11–30 June and 12–31 August. Data of the soil temperature were measured at a depth of 0.3 m below the earth surface and under the building foundation of the Philosophical Faculty of University of Ioannina. The floor area of this building was 2500 m^2. The floor and the external walls were made of 60 mm dense concrete, 40 mm expanded polystyrene insulation and 60 mm dense concrete. The density of dense concrete was equal to 2100 kg/m^3 while the density of the polystyrene was equal to 25 kg/m^3. The specific heat capacity of dense concrete was 833 J/kg°C while the specific heat capacity of the insulation was equal to 1014 J/kg°C. Accordingly, the thermal conductivity of the dense concrete was 1.40 W/m°C and the conductivity of the insulation was 0.03 W/m°C. The soil temperature data were recorded at 5 min intervals throughout the experiment. The ambient air temperature has been fluctuated during the experiments between 9.8 and 39.3°C.

The results of the experiments were compared with the theoretical calculations. Figures 4 and 5 show the temporal variations of the measured and of the calculated soil temperature for the time periods 11–30 June and 12–31 August, respectively. As it can be seen from these figures there is a very good agreement between the predicted and measured values. Moreover, Fig. 6 compares the observed with the calculated soil temperature values for the whole time period of the two experiments. As shown, there is a very good agreement between the theoretical and the measured data while their maximum rarely exceeds 0.3°C.

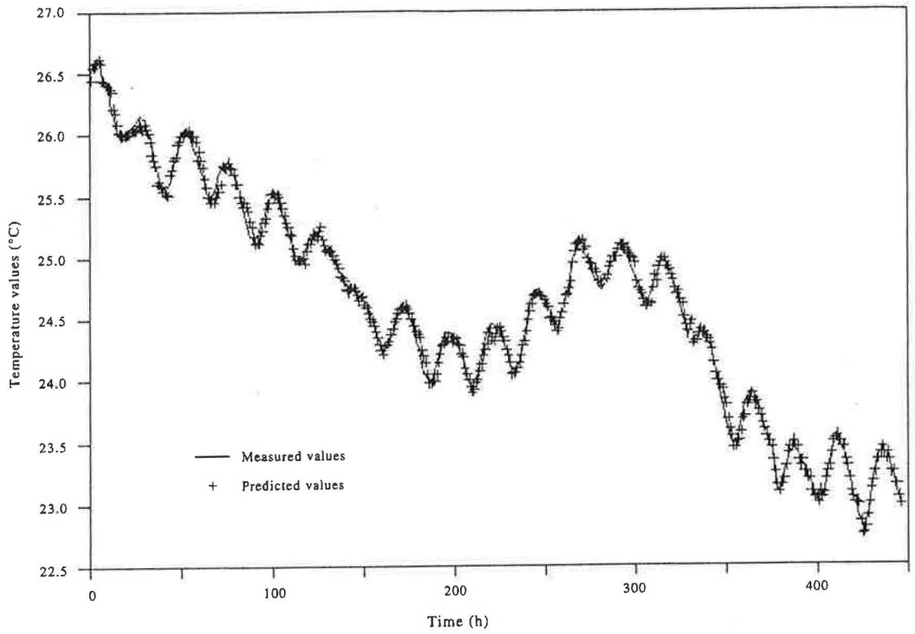

Fig. 4. The temporal variation of the measured and calculated soil temperature values for the time period 11–30 June.

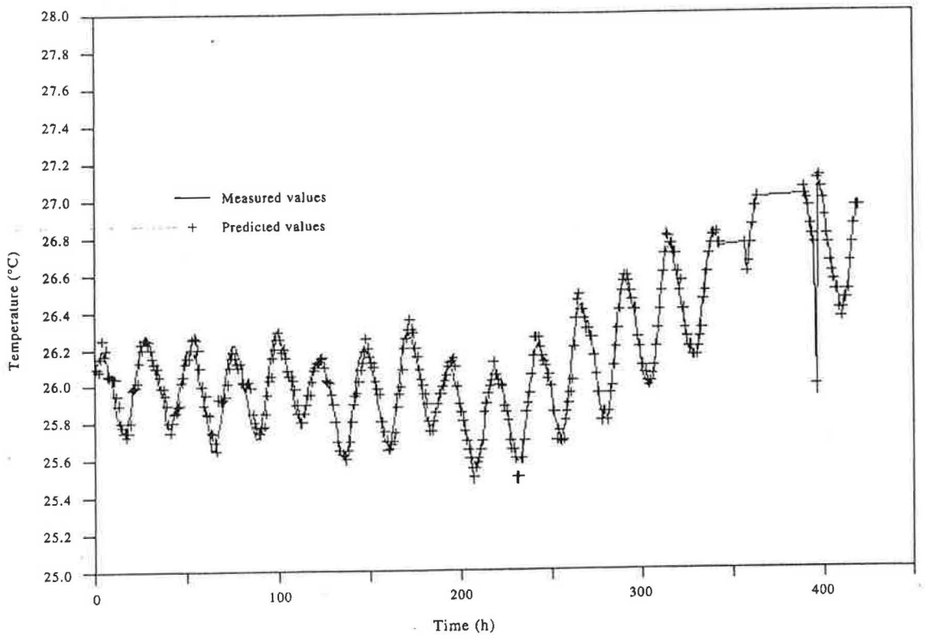

Fig. 5. The temporal variation of the measured and calculated soil temperature values for the time period 12–31 August.

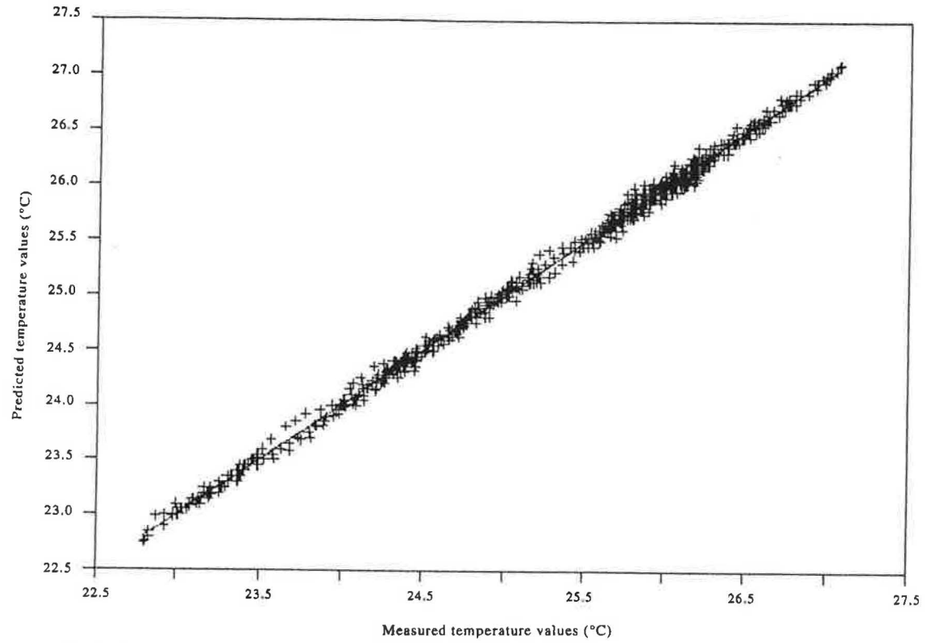

Fig. 6. Comparison between the observed with the calculated soil temperature values for the whole time period.

CONCLUDING REMARKS

An accurate, transient, implicit numerical model has been developed to calculate the ground temperature at various depths under a building foundation. The basic, three-dimensional thermal problem concerns homogeneous ground, constant indoor temperature and an outdoor temperature presenting a large temporal variability. The proposed model was validated against experimental data and it was found that it could accurately predict the temperature of the soil under a building foundation.

NOMENCLATURE

C_p specific heat capacity (J/kg°C)
K soil thermal conductivity (W/m°C)
K_i the thermal conductivity corresponding to grid point I (W/m°C)
Q heat flow to the ground (W)
S_i notation for the surface foundation against the ground (m^2)
t time (s)
t_p time period for outdoor periodic temperature (s)
T temperature in the soil (°C)
$T_{boundary}$ temperature at the boundary (°C)
T_i indoor temperature (°C)
T_L the temperature of the grid L (°C)
T_n amplitude of the temperature wave at the ground surface (°C)
T_0 annual mean temperature at the ground surface (°C)
$T_{out}(t)$ outdoor temperature (°C)
T_p^0 the old value (at time t) of the variable (°C)
$T_u(z)$ the undisturbed soil temperature, which is not influenced by the building presence (°C)
x,y horizontal Cartesian co-ordinates (m)
z vertical Cartesian co-ordinate (m)

Greek characters

Δx x-direction width of the control volume (m)
Δy y-direction width of the control volume (m)
Δz z-direction width of the control volume (m)
δx x-direction distance between two adjacent grid points (m)
δy y-direction distance between two adjacent grid points (m)
δz z-direction distance between two adjacent grid points (m)
ρ soil density (kg/m^3)
λ_n phase for periodic temperature

Subscripts

B neighbour in the z-direction (bottom)
b control-volume face between P and B
E neighbour in the positive x-direction (east side)
e control-volume face between P and E
N neighbour in the positive y-direction (north side)
n control-volume face between P and N
P central grid point under consideration
S neighbour in the negative y-direction (south side)
s control-volume face between P and S
T neighbour in the positive z-direction (top)
t control-volume face between P and T
W neighbour in the negative x-direction (west side)
w control-volume face between P and W